

# Hydrodynamic description of direct photon spectra and elliptic flow in Pb+Pb collisions at LHC

Sándor Lökös<sup>1,3</sup>, Gábor Kasza<sup>2,3</sup>

<sup>1</sup>*Institute of Nuclear Physics Polish Academy of Sciences, Kraków PL-31-342, Poland*

<sup>2</sup>*HUN-REN Wigner Research Centre for Physics, Budapest H-1121, Hungary*

<sup>3</sup>*Hungarian University of Agriculture and Life Sciences, Gyöngyös H-3200, Hungary*

March 21, 2024

## Abstract

In high energy heavy ion collisions a new state of matter, the strongly coupled quark gluon plasma is formed that exhibits the similar properties as our Universe had just a couple of microseconds after the Big Bang, hence such collisions are usually referred as Little Bangs. Subsequent investigations showed that the created medium is a nearly perfect fluid whose time evolution can be described by hydrodynamic models. The distribution of the hadrons that are created in the freeze-out after a rapid expansion carry information about the final state. On the other hand, with penetrating probes, e.g., with direct photons, one can model the time evolution of the quark gluon plasma. In this paper, we present a hydrodynamic model that was inspired by an analytical solution of relativistic hydrodynamics, calculate the invariant transverse momentum spectrum and the elliptic flow of direct photons and compare our results to LHC ALICE data to obtain the value of the model parameters. Based on the the results we give an estimation for the initial temperature of the plasma.

## 1 Introduction

In the early 2000s, a series of RHIC experimental results proved that a new, strongly coupled plasma, the quark gluon plasma (QGP) was created in heavy ion collisions [1–5]. It was also determined that in this medium, the mean free path of the quarks is very small [6] and its kinematic viscosity is close to the theorized minimum [7, 8] hence relativistic perfect fluid models can be utilized to describe its time evolution as Landau has proposed in 1953 [9]. The reason for the wide applicability of hydrodynamics is that it has no internal physical scale: hydrodynamics can be applied from the femtometre distances of the particles to the largest scales of the Universe.

Hadron spectra measured in heavy ion experiments carry information about the final state of the hot and dense hadronic medium but do not provide information about the time evolution of the quark-gluon plasma before the kinetic freeze-out [10]. We note that information about the phase after the chemical freeze-out but before the kinetic freeze-out might be accessible

by measuring resonance ratios, see e.g. in Refs. [11–13]. However, the length of this period is debated, but thermal models suggest that the chemical and the kinetic freeze-out of the hot and dense hadronic matter are two very close events in space-time, see for example Refs. [14, 15].

Direct photon measurements can be considered as penetrating probes that can be utilized to observe the evolution of the medium. Direct photons are created during the whole evolution and they can reach the detectors without considerable interaction with the plasma since they do not couple strongly only electromagnetically and the cross section for such processes is small. Hence they are an excellent probe to understand the time evolution of the QGP. Their spectrum is dominated by photons originated from hard scattering processes at high  $p_T$  and mostly thermal photons at low  $p_T$ . Therefore the hydrodynamic calculations are considered to be valid for the lower  $p_T$  region, however, there is room for access of photons from other sources to this region too [16–19].

Direct photon spectra were measured by WA98 [20], PHENIX [21–24] and ALICE [25]. Direct photon flow was measured in PHENIX [26] and ALICE [27]. Latter measurements attract great theoretical interest. The elliptic flow coefficient ( $v_2$ ) of direct photons is of the same order of magnitude as for hadrons that is usually referred to as *direct photon puzzle*. Indeed, it is not well understood that how the strong photon emission at the early stages has as large  $v_2$  as hadrons that are emitted at the later and cooler stage. The theoretical models that are compared to data cannot give a satisfactory description of the spectrum and the elliptic flow of direct photons at the same time [19, 28, 29].

In this manuscript, we calculate the direct photon spectra and the  $v_2$  elliptic flow coefficient based on a 1+3 dimensional boost-invariant perfect fluid hydrodynamic solution [30]. We note that previously, using the above mentioned hydrodynamic solution of Ref. [30], direct photon spectra and the  $v_2$  flow parameter have been calculated analytically in Ref. [31]. The calculation was performed using a second-order saddle-point approximation, and the resulting analytical formulae gave a statistically acceptable description of the direct photon spectrum measured by the PHENIX collaboration [32]. More recently, an analytical formula for the thermal contribution of the direct photon spectrum was derived from a 1+1 dimensional hydrodynamic solution characterized by a locally accelerating velocity field [33]. Comparing this analytical formula with the most recent spectrum of nonprompt direct photons measured by PHENIX [24], the scaling behaviour of the direct photon spectrum was observed. However, this result is based on a 1+1 dimensional solution of perfect fluid hydrodynamics, hence the  $v_2$  elliptic flow was not examined.

The success of the analytical hydrodynamic models motivated us to compare our calculations with the ALICE Pb+Pb at 2.76 TeV data [25, 27], with the aim of getting closer to solving the direct photon puzzle.

## 2 The hydrodynamic model

A hydrodynamic model is defined by a source function that gives a parametrization of the spatio-temporal distribution of the created medium in the final state. That is usually taken to be the Bose-Einstein distribution on the four dimensional hypersurface that is parametrized by the Cooper-Frye flux term:

$$S(x, p)d^4x = \frac{g}{(2\pi\hbar)^3} \frac{H(\tau)}{\tau_R} \frac{d\Sigma_\mu p^\mu}{\exp\left(\frac{p^\mu u_\mu}{T}\right) - 1}, \quad (1)$$

where  $g$  is the degeneracy factor,  $p^\mu$  is the four-momentum of the photons,  $u_\mu$  is the four-velocity of the fluid,  $\tau_R$  is the characteristic time of the particle emission in the momentum space and  $H(\tau)$  is a proper-time dependent window-, or opacity-function [34] that we shall discuss later. The  $d\Sigma_\mu p^\mu$  term is called Cooper-Frye factor of the particle flux [35], where  $d\Sigma_\mu$  gives the normal vector of the hypersurface that is assumed to be parallel with the four-velocity, i.e.

$$d\Sigma^\mu = u^\mu dt d^3x. \quad (2)$$

The  $H(\tau)$  function describes the proper-time distribution of the opacity of the medium to photons. The photons are created continuously in the QGP and they do not participate in the strong interaction, thus their mean free path could be larger than the size of the thermalized fireball. Accordingly,  $H(\tau)$  corresponds to the proper time duration of the thermal radiation, the time between the thermalization ( $\tau_0$ ) and the freeze-out ( $\tau_f$ ):

$$H(\tau) = \Theta(\tau - \tau_0) - \Theta(\tau - \tau_f). \quad (3)$$

With this form of  $H(\tau)$ , the source function can be written as

$$S(x, p) d^4x = \frac{g}{(2\pi\hbar)^3} \frac{\Theta(\tau - \tau_0) - \Theta(\tau - \tau_f)}{\tau_R} p^\mu u_\mu \exp\left(\frac{p^\mu u_\mu}{T}\right) dt d^3x. \quad (4)$$

Let us introduce the constant normalization factor as  $\mathcal{N} = \frac{g}{(2\pi\hbar)^3} \frac{1}{\tau_R}$ . The velocity field is taken to be a Hubble flow, i.e.

$$u_\mu = \gamma(1, \mathbf{v}) = \gamma\left(1, \frac{\mathbf{r}}{t}\right), \quad (5)$$

where  $\mathbf{v}$  is the three-velocity,  $\mathbf{r}$  is the three dimensional position vector and  $t$  is the coordinate time. The Lorentz-factor is denoted by  $\gamma$ .

In this paper, we describe the invariant transverse momentum distribution and the elliptic flow of the direct photons therefore we give the model in cylindrical spatial coordinates that suit better the geometry of the system than the Cartesian coordinates. The two sets of coordinates are related as  $r = \sqrt{r_x^2 + r_y^2}$ ,  $\alpha = \arctan(r_y/r_x)$ . Hence the position and momentum four-vectors have the form as

$$x_\mu = (t, r, \alpha, r_z), \quad p_\mu = (E, p_T \cos(\phi), p_T \sin(\phi), p_z) \quad (6)$$

where  $r$  is the radial coordinate,  $\alpha$  is the spatial azimuth angle,  $r_z$  is the coordinate in the beam direction,  $E$  is the photon's energy,  $p_T$  is the transverse momentum,  $\phi$  is the momentum azimuth angle and  $p_z$  is the longitudinal component of the momentum. Taking into account for the limited pseudorapidity acceptance of the ALICE detector ( $|\eta| < 0.8$ ) further simplification can be made as  $p_z \approx 0$ . Therefore, in cylindrical coordinates,

$$p^\mu u_\mu \approx p_T \gamma [1 - r/t \cos(\phi - \alpha)], \quad (7)$$

that gives the final form of the source function as

$$\begin{aligned} S(t, r, \alpha, r_z, p_T, \phi) dt r d\alpha dr dr_z = \\ = \mathcal{N} r p_T H(\tau) \gamma [1 - r/t \cos(\phi - \alpha)] \exp\left(-\frac{p_T \gamma [1 - r/t \cos(\phi - \alpha)]}{T}\right) dt dr d\alpha dr_z, \end{aligned} \quad (8)$$

where, for now, we give all the arguments. Observable quantities, like the invariant momentum distributions or the elliptic flow, can be obtained by integrating and calculating the space-time

moments of the source function. The invariant momentum distribution is given as (taken at mid-rapidity:  $y = 0$ )

$$N_1(p_T, \phi) = E \left. \frac{d^3 N}{dp^3} \right|_{p_z=0} = \left. \frac{d^3 N}{d\phi dp_T dy} \right|_{y=0} = \int S(t, r, \alpha, r_z, p_T, \phi) dt r d\alpha dr dr_z. \quad (9)$$

One of the observable quantities we calculate is the transverse momentum distribution at mid-rapidity. It can be calculated from the invariant momentum distribution by integrating  $N_1(p_T, \phi)$  with respect to the azimuth angle:

$$\left. \frac{d^2 N}{p_T dp_T dy} \right|_{y=0} = \int_0^{2\pi} d\phi N_1(p_T, \phi). \quad (10)$$

The anisotropies of the invariant momentum distribution function are defined as  $n$ -th order Fourier coefficients with respect to the angle of the  $n$ -th order event plane. In this paper, we restrict ourselves to investigate the second order anisotropies:

$$v_2(p_T) = \frac{\int_0^{2\pi} d\phi \cos(2\phi) N_1(p_T, \phi)}{\int_0^{2\pi} d\phi N_1(p_T, \phi)}. \quad (11)$$

### 3 Temperature profile

In the source function defined in Eq. (8), the temperature has to be specified. In this work, the temperature is given by an exact and analytic, self-similar solution of perfect fluid hydrodynamics based on Ref. [30]. Although this solution was found with finite chemical potential, in this manuscript we describe the medium at zero chemical potential. In such a medium, defining conserved particle number is problematic due to the continuously created and annihilated virtual particles, so the solution used in this manuscript can be given by the temperature and the entropy density with the equation of state  $\varepsilon = \kappa p$ , where  $\kappa$ , in general, can be the function of the temperature.

The spatial anisotropy can be introduced into this hydrodynamic model by the so-called scale variable, which satisfies the  $u^\mu \partial_\mu s = 0$  equation. In the case of an elliptic fireball it can be written in elliptical coordinates as

$$s = \frac{r^2}{R^2} (1 + \epsilon_2 \cos(2\alpha)) + \frac{r_z^2}{Z^2}, \quad (12)$$

where the parameters  $R$  and  $\epsilon_2$  are related to the axis of the ellipsoid in the Cartesian system as

$$\frac{1}{R^2} = \left( \frac{1}{X^2} + \frac{1}{Y^2} \right), \quad \epsilon_2 = \frac{Y - X}{Y + X}. \quad (13)$$

The scales are denoted by  $X, Y$  and  $Z$ , and they stand for the time dependent axes of the fireball. Here we use  $X(t) = \dot{X}_0 t$ ,  $Y(t) = \dot{Y}_0 t$  and  $Z(t) = \dot{Z}_0 t$  as described in the boost-invariant solution of Ref. [30]. The  $s$  dependence of the temperature is carried by an arbitrary function  $\mathcal{T}(s)$ , so in our model the temperature is factorized into the function  $\mathcal{T}(s)$  and a

homogeneous term as  $T(\tau, s) = T_H(\tau)\mathcal{T}(s)$ . This is due to the definition of  $s$  which is given by the  $u^\mu \partial_\mu s = 0$  equation, thus the  $s$  dependence in the temperature is eliminated from the equation of energy conservation [30]. If the velocity field of the fluid is defined by Eq. (5) and the EoS is written as  $\varepsilon = \kappa p$ , the solution of the temperature can be calculated from the following differential equation, which corresponds to the energy conservation:

$$\left[ (1 + \kappa) \frac{d}{dT} \left( \frac{\kappa T}{1 + \kappa} \right) \right] \frac{\partial T}{\partial \tau} + \frac{3T}{\tau} = 0. \quad (14)$$

This differential equation can be solved in three cases:

1. The temperature depends only on  $\tau$  and  $\kappa$  can be temperature dependent:  $T \equiv T(\tau)$ ,  $\mathcal{T}(s) = 1$ ,  $\kappa \equiv \kappa(T)$ .
2. The coefficient of the derivative of  $T$  in Eq. (14) is fixed to a constant, so the temperature can depend both on  $\tau$  and  $s$ , and  $\kappa$  is a temperature dependent function which is given in Ref. [36].
3. The temperature can depend on both  $\tau$  and  $s$ , but  $\kappa$  has to be independent from the temperature:  $T(\tau, s)$ ,  $\kappa = \text{constant}$ .

The first option has the benefit that it allows us to incorporate the lattice QCD EoS, e.g., that was published in Ref. [37] into our calculations. However, in this case, Eq. (14) allows only the  $\tau$  dependence of the temperature, so there is no spatial decay of the temperature of the fireball. This case does not give a satisfactory description of the measured spectra of thermal radiation. We note that an implicit hydrodynamic solution was derived using a class of EoS that includes the lattice QCD EoS [38].

The second option allows one to introduce spatially decreasing profile for the temperature using the arbitrary function  $\mathcal{T}(s)$ , and in this case too, the equation of state belongs to the same class as the equation of state of the lattice QCD. However, the form of  $\kappa(T)$  is then fixed and only applicable over a certain range of temperature, as discussed in Ref. [36].

In the third option,  $\kappa$  can only be a temperature-independent constant, which can be considered as a value averaged over the temperature. In the nonrelativistic limit of the solution discussed here, we observed that the application of the temperature dependent EoS has a negligible effect in the fireball expansion dynamics, so we fixed  $\kappa$  to the temperature-averaged value based on the lattice result [37], that is  $\kappa = 3.75$ , and utilize the solution for the temperature from Ref. [30] in the form of

$$T(\tau, s) = T_f \left( \frac{\tau_f}{\tau} \right)^{3/\kappa} \mathcal{T}(s). \quad (15)$$

Here  $T_f$  is the freeze-out temperature and  $\tau_f$  is the freeze-out proper time. Since we consider vanishing bariochemical potential, the constant proportionality factor  $\kappa$  between the pressure and energy density is equal to the inverse square of the speed of sound:  $\kappa = c_s^{-2}$ . The scaling function,  $\mathcal{T}(s)$ , is arbitrary and here taken to have a Gaussian profile:

$$\mathcal{T}(s) = \exp(-bs/2), \quad (16)$$

where we introduced a new model parameter,  $b$ , which is an arbitrary positive real number.

## 4 Model comparison to ALICE data

Observables that can be calculated from the model and compared to data are described above in Eq. (10) and Eq. (11). Because of the rather complicated dependence on the coordinates, numerical integration is employed. However, in the same model we use, Eq. (10) and Eq. (11) have been analytically integrated earlier in Refs. [31,39], but only at the cost of several reasonable approximations.

Direct photon measurements are experimentally challenging hence a limited amount of data is available. We choose to compare our model calculations to single particle transverse momentum [25,40] and elliptical flow [27,41] data simultaneously that were measured by ALICE at  $\sqrt{s_{NN}} = 2.76$  TeV in Pb+Pb collisions [27].

We compare our calculations to the data by standard  $\chi^2$  minimization method employing ROOT Minuit2 package [42]. Only the statistical uncertainties of the data are considered in the minimization process. To reach sufficient precision in the numerical integration, considerable amount of computational time was necessary therefore we restrict our fit to four parameters, namely, to the freeze-out temperature  $T_f$ , freeze-out proper-time  $\tau_f$ , ellipticity  $\epsilon_2$  and normalization  $\mathcal{N}$  as it is listed in Tab. 1. The remaining parameters were fixed to values that are available in the literature, e.g., in Ref. [31]. The statistical uncertainties of the fit parameters were determined by Minuit2 package.

We also determined the systematic uncertainties of our choice of the fixed parameters. The systematic checks were done as follows: we redo the fits by changing the value of one of the fixed parameters up or down at a time by  $\sim 10\%$  and obtain new values for the fit parameters as alternative ones. Then we calculate the relative deviation of the alternative values from the default one.

The largest contribution to the systematic uncertainties is given by the variation of the  $\kappa$  parameter. It is observed that larger  $\kappa$  value, which corresponds to softer EoS, implies higher initial and freeze-out temperatures. On the other hand, the ellipticity parameter and the freeze-out proper time are not sensitive depends on the value of the  $\kappa$  parameter. As it is discussed in Sec. 3, we utilized temperature-independent  $\kappa$  in our model. We cross-checked the choice of the temperature averaged value by fitting  $\kappa$  instead of  $\epsilon_2$  that is the least sensitive to the variation of the  $\kappa$ . We fixed the value of  $\epsilon_2$  to the one that comes from the default fit and the same was done for the other previously fixed model-parameters too. By repeating the fit, we have found that the values of the fit parameters are modified around 2-3% when  $\kappa$  is fitted instead of  $\epsilon_2$ . Accordingly, we have concluded that  $\kappa = 3.75$ , which corresponds to the temperature-averaged value of the lattice QCD EoS [37], is in agreement with the spectrum and the  $v_2$  elliptic flow of direct photons measured in Pb+Pb at  $\sqrt{s_{NN}} = 2.76$  GeV collisions.

The total systematical uncertainties of the fit parameters then were calculated by summing up all the relative deviations in quadrature. The parameters could be correlated. The described method of determination of the systematic uncertainties can be regarded as a conservative estimate.

Our fit results are shown in Fig. 1 for the spectrum and in Fig. 2 for the elliptic flow. We also summarize the fit results in Tab. 1.

Parameter	Fit value	Stat. uncert.	Syst. uncert.
$T_f$ [MeV]	143.6	0.8	35.0
$\tau_f$ [fm]	7.92	0.57	1.83
$\epsilon_2$	0.24	0.01	0.13
$\mathcal{N}$	3.01	0.63	2.66
$\dot{R}_0$	0.20	const.	const.
$\dot{Z}_0$	0.15	const.	const.
$b$	0.10	const.	const.
$\kappa$	3.75	const.	const.

Table 1: Obtained parameter values from the simultaneous fit to the ALICE data of direct photon spectrum [25] and direct photon elliptic flow [27]. The fixed parameters are indicated with (const.) in the Stat. uncertainty column. The systematical uncertainties are determined based on fits with fixed parameters varied by  $\sim \pm 10\%$  around their nominal value.

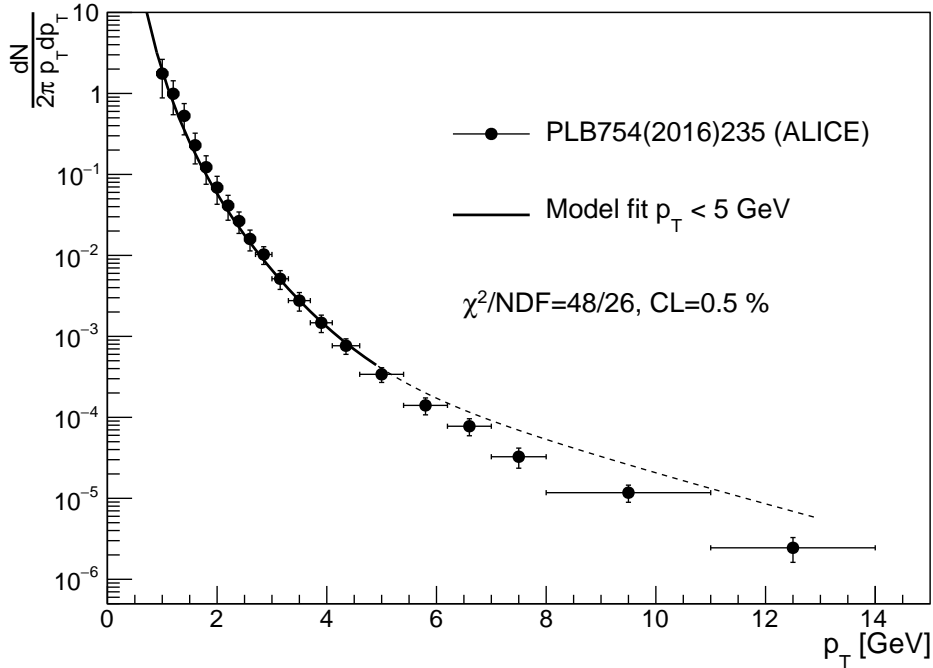


Figure 1: Model fit to the direct photon spectrum measured by the ALICE Collaboration [25,40]. The fit was made simultaneously for the spectrum and the elliptic flow shown in Fig. 2. The solid line denotes the range where the fit was constrained, the dashed line demonstrates the fit function on the whole range of available data.

## 5 Discussion

Our simple hydrodynamic model gives a statistically acceptable simultaneous description of the  $p_T$ -spectrum and the elliptic flow of direct photons in ALICE Pb+Pb at 2.76 collisions in terms of  $\chi^2/\text{NDF}$ , even beyond the expected limit of validity of the hydro description that is usually considered to be  $p_T < 2 - 3$  GeV. Our model is compatible with the data up to  $p_T < 5$  GeV, however, we note that the rather large uncertainties of the elliptic flow data prevents a strong conclusion.

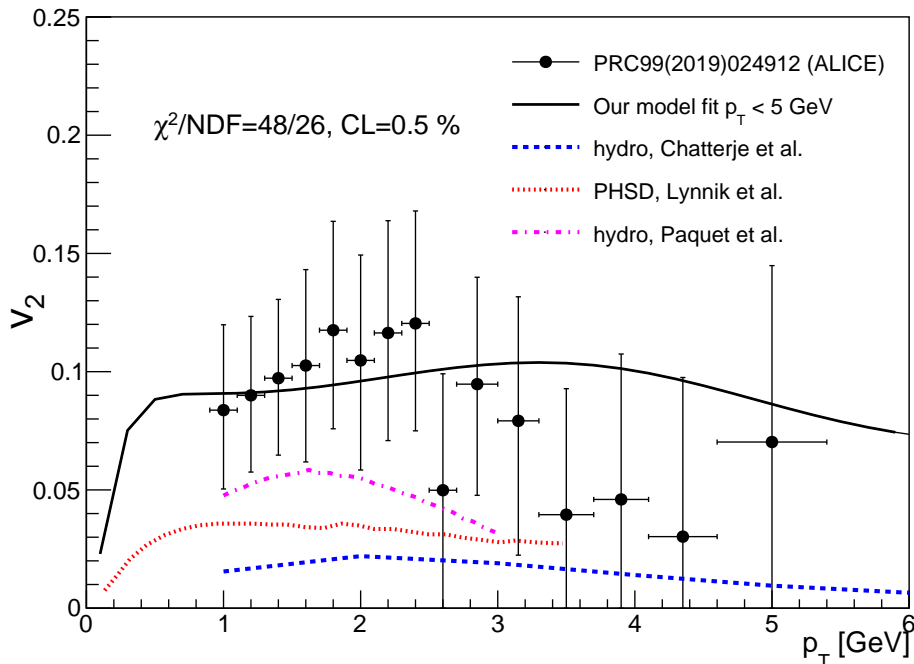


Figure 2: Model fit of the direct photon elliptic flow measured by the ALICE Collaboration [27, 41]. The fit was made simultaneously for the spectrum and the elliptic flow shown in Fig. 1. The solid line denotes our model fit. The dashed lines are different models from the ALICE publication [19, 28, 29].

In Fig. 2, we have compared our description of  $v_2$  with other hydrodynamic calculations [28, 29] and a transport model [19], that were included into the ALICE publication [27]. Our calculations show better agreement with the data, however the large uncertainties of the experimental data allow to draw conclusions only on the qualitative level.

Based on the temperature profile that we described in Section 3, we were able to determine the initial temperature of the plasma in the center of the fireball, that is

$$T_{\text{init}}=T(\tau=1)=751.9\pm 44.0(\text{stat})\pm 230.1(\text{syst})\text{MeV}. \quad (17)$$

This result for the initial temperature is clearly higher than the Hagedorn temperature, even if we take into account that theoretical predictions give a wide range for the Hagedorn temperature [43–46]. Hence we conclude that the medium created in Pb+Pb at  $\sqrt{s_{NN}}=2.76$  TeV collisions cannot be interpreted by a description involving hadrons only. In addition, we note that our results provide values for the initial and freeze-out temperatures (or equivalently for the initial and freeze-out proper times) that are compatible with the results of other analyses on hadronic [47, 48] and direct photon [31, 33, 39, 49–51] observables.

## 6 Summary

In our studies, we investigate the applicability of the hydrodynamic description of the direct photon data measured by ALICE experiments at LHC. In our model, we utilized the temperature-averaged lattice QCD equation of state with an exact and analytical solution of



relativistic hydrodynamics. We found a good agreement between the data and the model with realistic parameters. We were able to determine the initial temperature of the fireball. Our model calculations are closer to the data than the referred approaches that we adopt from the experimental paper.

## 7 Acknowledgement

This research was funded by the NKFIH grants K-138136 and K-147557, and the KKP-2024 Research Excellence Programme of MATE, Hungary.

## References

- [1] PHENIX, K. Adcox *et al.*, Phys. Rev. Lett. **88**, 022301 (2002), nucl-ex/0109003.
- [2] PHENIX, K. Adcox *et al.*, Phys. Rev. Lett. **86**, 3500 (2001), nucl-ex/0012008.
- [3] STAR, C. Adler *et al.*, Phys. Rev. Lett. **87**, 112303 (2001), nucl-ex/0106004.
- [4] PHENIX, S. S. Adler *et al.*, Phys. Rev. Lett. **91**, 072303 (2003), nucl-ex/0306021.
- [5] PHENIX, S. S. Adler *et al.*, Phys. Rev. Lett. **91**, 072301 (2003), nucl-ex/0304022.
- [6] PHENIX, S. S. Adler *et al.*, Phys. Rev. Lett. **91**, 182301 (2003), nucl-ex/0305013.
- [7] PHENIX, A. Adare *et al.*, Phys. Rev. Lett. **98**, 172301 (2007), nucl-ex/0611018.
- [8] PHENIX, A. Adare *et al.*, Phys. Rev. Lett. **105**, 062301 (2010), 1003.5586.
- [9] L. D. Landau, Izv. Akad. Nauk Ser. Fiz. **17**, 51 (1953).
- [10] M. Csanad, Acta Phys. Polon. B **40**, 1193 (2009), 0903.1278.
- [11] S. Lokos and B. Tomasik, Phys. Rev. C **106**, 034912 (2022), 2206.11300.
- [12] A. G. Knospe, C. Markert, K. Werner, J. Steinheimer, and M. Bleicher, Phys. Rev. C **93**, 014911 (2016).
- [13] H. Bebie, P. Gerber, J. Goity, and H. Leutwyler, Nuclear Physics B **378**, 95 (1992).
- [14] W. Broniowski and W. Florkowski, Phys. Rev. Lett. **87**, 272302 (2001), nucl-th/0106050.
- [15] W. Broniowski, A. Baran, and W. Florkowski, Acta Phys. Polon. B **33**, 4235 (2002), hep-ph/0209286.
- [16] G. m. c. Başar, D. E. Kharzeev, and V. Skokov, Phys. Rev. Lett. **109**, 202303 (2012).
- [17] G. m. c. Başar, D. E. Kharzeev, and E. V. Shuryak, Phys. Rev. C **90**, 014905 (2014).
- [18] C. Gale, J.-F. m. c. Paquet, B. Schenke, and C. Shen, Phys. Rev. C **105**, 014909 (2022).
- [19] O. Linnyk, V. Konchakovski, T. Steinert, W. Cassing, and E. L. Bratkovskaya, Phys. Rev. C **92**, 054914 (2015).
- [20] WA98, M. M. Aggarwal *et al.*, Phys. Rev. Lett. **85**, 3595 (2000), nucl-ex/0006008.
- [21] PHENIX Collaboration, S. S. e. a. Adler, Phys. Rev. Lett. **94**, 232301 (2005).
- [22] PHENIX Collaboration, A. e. a. Adare, Phys. Rev. Lett. **104**, 132301 (2010).
- [23] PHENIX Collaboration, S. e. a. Afanasiev, Phys. Rev. Lett. **109**, 152302 (2012).
- [24] PHENIX, U. A. Acharya *et al.*, (2022), 2203.17187.
- [25] ALICE, J. Adam *et al.*, Phys. Lett. B **754**, 235 (2016), 1509.07324.
- [26] PHENIX Collaboration, A. e. a. Adare, Phys. Rev. Lett. **109**, 122302 (2012).

- [27] ALICE, S. Acharya *et al.*, Phys. Lett. B **789**, 308 (2019), 1805.04403.
- [28] C. Gale *et al.*, Phys. Rev. Lett. **114**, 072301 (2015).
- [29] R. Chatterjee, P. Dasgupta, and D. K. Srivastava, Phys. Rev. C **96**, 014911 (2017).
- [30] T. Csorgo, L. P. Csernai, Y. Hama, and T. Kodama, Acta Phys. Hung. A **21**, 73 (2004), nucl-th/0306004.
- [31] M. Csanad and I. Majer, Central Eur. J. Phys. **10**, 850 (2012), 1101.1279.
- [32] PHENIX, A. Adare *et al.*, Phys. Rev. Lett. **109**, 122302 (2012), 1105.4126.
- [33] G. Kasza, (2023), 2311.03568.
- [34] T. Csorgo, Acta Phys. Hung. A **15**, 1 (2002), hep-ph/0001233.
- [35] F. Cooper and G. Frye, Phys. Rev. D **10**, 186 (1974).
- [36] T. Csörgő and G. Kasza, New exact solutions of hydrodynamics for rehadronizing fireballs with lattice QCD equation of state, in *24th Low-x Meeting*, 2016, 1610.02197.
- [37] S. Borsanyi *et al.*, JHEP **11**, 077 (2010), 1007.2580.
- [38] M. Csanád, M. I. Nagy, and S. Lökös, Eur. Phys. J. A **48**, 173 (2012), 1205.5965.
- [39] M. Csanad and I. Majer, Phys. Part. Nucl. Lett. **8**, 1013 (2011), 1101.1280.
- [40] ALICE Collaboration, Direct photon production in Pb-Pb collisions at  $\sqrt{s_{NN}} = 2.76$  TeV, HEPData (collection), 2016, <https://doi.org/10.17182/hepdata.73093>.
- [41] ALICE Collaboration, Direct photon elliptic flow in Pb-Pb collisions at  $\sqrt{s_{NN}} = 2.76$  TeV, HEPData (collection), 2019, <https://doi.org/10.17182/hepdata.88050>.
- [42] R. Brun and F. Rademakers, Nucl. Inst. & Meth. in Phys. Res. A **389**, 81 (1997).
- [43] W. Broniowski and W. Florkowski, Phys. Lett. B **490**, 223 (2000), hep-ph/0004104.
- [44] W. Broniowski, W. Florkowski, and L. Y. Glozman, Phys. Rev. D **70**, 117503 (2004), hep-ph/0407290.
- [45] T. D. Cohen and V. Krejcirik, J. Phys. G **39**, 055001 (2012), 1107.2130.
- [46] J. Cleymans and D. Worku, Mod. Phys. Lett. A **26**, 1197 (2011), 1103.1463.
- [47] M. Csanad and M. Vargyas, Eur. Phys. J. A **44**, 473 (2010), 0909.4842.
- [48] J. Ze-Fang, Y. Chun-Bin, M. Csanad, and T. Csorgo, Phys. Rev. C **97**, 064906 (2018), 1711.10740.
- [49] PHENIX, A. Adare *et al.*, Phys. Rev. Lett. **104**, 132301 (2010), 0804.4168.
- [50] J. K. Nayak, J.-e. Alam, S. Sarkar, and B. Sinha, J. Phys. G **35**, 104161 (2008), 0806.0447.
- [51] J. K. Nayak and B. Sinha, Phys. Lett. B **719**, 110 (2013), 1210.3993.